

# Catalytically active self-assembled silica-based nanostructures containing supported nanoparticles

Camino Gonzalez-Arellano,<sup>a</sup> Alina Mariana Balu,<sup>b</sup> Rafael Luque<sup>\*a,b</sup> and Duncan J. Macquarrie<sup>a</sup>

Received 2nd July 2010, Accepted 27th August 2010

DOI: 10.1039/c0gc00282h

Self-assembled tubular silica-based nanostructures can be prepared using a simple, low-energy intensive and benign protocol under mild conditions (<100 °C) using microwave irradiation and conventional heating. These nanotubes were found to contain metal nanoparticles that are catalytically active in the microwave-assisted homocoupling of terminal alkynes.

## Introduction

Nanomaterials have attracted a great deal of attention over the last few decades due to the importance of miniaturisation and nanotechnologies in key advances for a sustainable future. Sizes, shapes and surface properties can be designed to evoke specific nanomaterial functions with the aim to be utilised in a particular application/end use such as chemical sensors,<sup>1</sup> biomedicine,<sup>2</sup> optoelectronic devices<sup>3</sup> and catalysis.<sup>4</sup>

Nanotubes are a particularly interesting example of nanomaterials. These nanostructures have been reported in a remarkable number and variety of applications, using different chemical and physicochemical synthetic methodologies (*e.g.* vapor-, solution- and supercritical fluid-liquid-solid systems,<sup>5–7</sup> and surfactant-mediated sol–gel methods<sup>8</sup>). Nevertheless, reports of simple, low-energy intensive and benign methodologies are scarce, with multiple-steps, organic solvent-mediated and energy intensive methodologies being mostly reported for the preparation of nanotubular structures.<sup>5–9</sup> Well-developed silica nanotubes have been prepared using copper sulfide nanocrystals under supercritical toluene (500 °C, 10.3 MPa).<sup>9c</sup> In comparison to these systems, we recently reported the preparation of self-assembled nanotubular domains under both conventional heating and microwave irradiation in aqueous surfactant solutions.<sup>10</sup> To the best of our knowledge, these findings were the first report of the generation of such nanomaterials in water under mild synthesis conditions (<100 °C). These materials were also found to contain (metal) nanoparticles into their nanostructures.<sup>10</sup>

Supported nanoparticles on nanotubes have also been the subject of many investigations due to their important and interesting applications in catalysis.<sup>4,11</sup> However, most studies are limited to carbon nanotubes<sup>12</sup> and other nanotubular structures have rarely been reported to have broad catalytic applications.

In this work, we aim to report the structural and textural properties of self-assembled tubular nanostructures from aqueous surfactant solutions as well as their plausible mechanisms of

formation. Parameters such as the effect of the methodology of preparation, different metals and metal salt precursors utilised and the effect of the halide anions in the formation of the nanostructures have been investigated as well as their applications in the heterogeneously catalysed microwave-assisted homocoupling of terminal alkynes.

## Experimental

### Materials preparation

In the proposed synthesis of nanotubes (NT), 0.6 mmol *n*-dodecylamine (0.14 mL), 2 mmol tetraethoxyorthosilicate (TEOS, 0.45 mL), 0.2 g metal salt (*i.e.* FeCl<sub>2</sub>·4H<sub>2</sub>O, RuCl<sub>3</sub>·xH<sub>2</sub>O, CuCl<sub>2</sub>·2H<sub>2</sub>O, NiCl<sub>2</sub>·6H<sub>2</sub>O and CoCl<sub>2</sub>·6H<sub>2</sub>O), 2 mL water and 2 mL acetonitrile were added to a microwave tube and microwaved for 1 to 15 min at 200 W (maximum temperature reached 80–110 °C depending on the material). Materials were denoted as metal-Microwave Induced NanoTubes (metal-MINT; *e.g.* Cu-MINT). Alternatively, the preparation of NT was carried out under conventional heating (70 °C), under identical conditions to those reported in the microwave protocol, to compare results. These materials were simply denoted as metal-NanoTubes (*e.g.* copper nanotubes). The resultant coloured solid was filtered off, thoroughly washed with acetonitrile and acetone and dried overnight at 100 °C before extracting the template in refluxing ethanol (5 h). Materials were then oven dried (100 °C) overnight and further characterised.<sup>10</sup>

### Characterisation

Materials were characterised by means of several techniques including Scanning Electron Microscopy (SEM), Transmission Electron Microscopy (TEM), Nitrogen physisorption and X-Ray Photoelectron Spectroscopy (XPS).

SEM micrographs were recorded in a JEOL JSM-6490LV. Samples were Au/Pd coated on a high resolution sputter SC7640 at a sputtering rate of 1500V per minute, up to 7 nm thickness.

TEM micrographs were recorded on a FEI Tecnai G2 fitted with a CCD camera for ease and speed of use. The resolution is around 0.4 nm. Samples were suspended in ethanol and deposited straight away on a copper grid prior to analysis.

Nitrogen adsorption measurements were carried out at 77 K using an ASAP 2010 volumetric adsorption analyzer from

<sup>a</sup>Green Chemistry Centre Of Excellence, The University of York, Heslington, York, UK, YO10 5DD

<sup>b</sup>Departamento de Química Orgánica, Universidad de Córdoba, Campus de Rabanales, Edificio Marie Curie, Ctra Nnal IV, Km 396, E14014, Córdoba, Spain. E-mail: q62alsor@uco.es; Fax: +34 957 212066; Tel: +34 957 211050

Micromeritics. The samples were outgassed for 2 h at 100 °C under vacuum ( $p < 10^{-2}$  Pa) and subsequently analyzed. The linear part of the BET equation (relative pressure between 0.05 and 0.22) was used for the determination of the specific surface area. Materials were found to be mostly microporous.

XPS (aka ESCA) measurements were performed in a ultra high vacuum (UHV) multipurpose surface analysis system (Specs™ model, Germany) operating at pressures  $< 10^{-10}$  mbar using a conventional X-Ray source (XR-50, Specs, Mg-K $\alpha$ , 1253.6 eV) in a “stop-and-go” mode to reduce potential damage due to sample irradiation. The survey and detailed Fe and Cu high-resolution spectra (pass energy 25 and 10 eV, step size 1 and 0.1 eV, respectively) were recorded at room temperature with a Phoibos 150-MCD energy analyser. Powdered samples were deposited on a sample holder using double-sided adhesive tape and subsequently evacuated under vacuum ( $< 10^{-6}$  Torr) overnight. Eventually, the sample holder containing the degassed sample was transferred to the analysis chamber for XPS studies. Binding energies were referenced to the C1s line at 284.6 eV from adventitious carbon. The curve deconvolution of the obtained XPS spectra were obtained using the Casa XPS program.

The metal content in the materials was determined using Inductively Coupled Plasma (ICP) in a Philips PU 70000 sequential spectrometer equipped with an Echelle monochromator (0.0075 nm resolution). Samples were digested in HNO<sub>3</sub> (Ru was removed using aqua regia) and subsequently analysed by ICP at the University of Newcastle.

### Catalytic tests

In a typical catalytic experiment, 4 mmol phenylacetylene, 2 mmol di-azabicyclo [2.2.2] octane (DABCO) and 0.05 g catalyst were microwaved in a CEM-DISCOVER microwave reactor under air for 15 min at 300 W (maximum power output). Dodecane was added to the mixture as internal standard. Upon reaction completion, aliquots of the final mixture were sampled and subsequently analysed by GC/MS using an Agilent 6980 N GC model fitted with a Petrocol capillary column and a FID detector. Experiments were conducted on a closed vessel (pressure controlled) under continuous stirring. The microwave method was generally power controlled where samples were irradiated with the maximum power output (300 W) and reached different temperatures in the 140–170 °C range.

### Results and discussion

Following our recently developed microwave protocol to synthesize a variety of supported nanoparticles on mesoporous materials at mild conditions,<sup>13,14</sup> we were prompted to investigate whether a direct one-pot synthesis involving simultaneous coprecipitation of the metal precursor and the silica gel could lead to embedded nanoparticles on a porous network. Having the possibility to explore a range of metal precursors, our preliminary aims were focused on cheap, readily available and environmentally friendly precursors such as Fe and Cu chlorides (FeCl<sub>2</sub> and CuCl<sub>2</sub>).

Thus, preliminary results of the simultaneous co-precipitation of these metal salts in *n*-dodecylamine/TEOS/water/ACN mix-

tures similar to those utilised for the preparation of mesoporous hexagonal silicas<sup>15</sup> pointed to the generation of supported nanoparticles on the surface of interestingly structured porous materials. Further investigations on such materials using SEM and TEM (Fig. 1 and Fig. 2) showed the formation of distinctive self-assembled nanotubular domains from the original synthesis gel, regardless of the metal precursor employed.

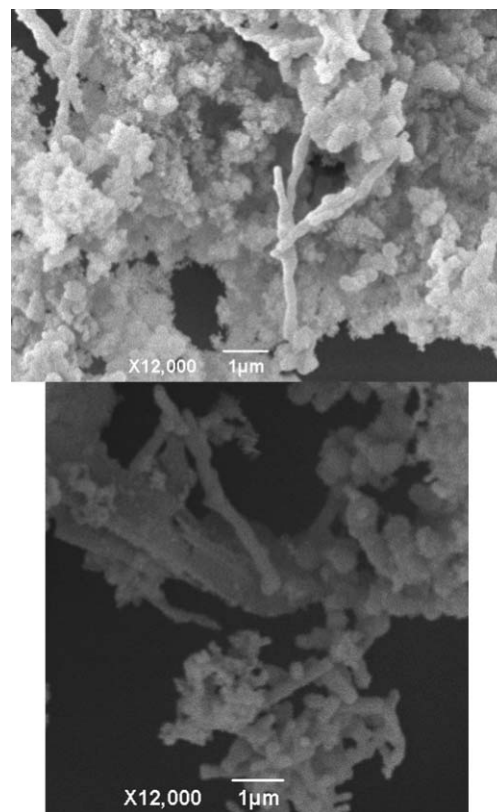


**Fig. 1** SEM micrographs of Ni-MINT (top) and Cu-MINT (bottom).

Nanotubular domains observed had sizes between 1 to several micrometres long with diameters typically between 0.1 to 5  $\mu\text{m}$  (Fig. 1). Tubular-shaped structures found in SEM were further confirmed in the TEM micrographs (Fig. 2). These images evidenced the presence of rod/tube-like shapes in the materials regardless of the mild synthetic methodology employed in their preparation (see experimental). Clear nanotubular/nanofibres exhibited in Fig. 2B pointed out these nanostructures were typically 100–500 nm long with diameters typically between 10–100 nm, in good agreement with those observed in the SEM micrographs.

Promisingly, the use of other metals including Ru, Ni and to some extent Co also rendered similarly developed tubular nanostructures.<sup>10</sup> The degree of development of the nanotubes network was found to follow the order:

Cu > Ru > Ni > Fe  $\gg$  Co with reasonably developed Cu, Ru and Ni MINT (Fig. 2). Nanoparticles on the nanostructures could be clearly observed in many cases (Fig. 3).

Metal content (as determined by elemental analysis) showed a ca. 0.5 wt% metal loading irrespective of the synthesis conditions and the metal employed (Table 1).

**Table 1** Textural properties [surface area (SBET,  $\text{m}^2 \text{g}^{-1}$ ), pore diameter (DBJH, nm), pore volume (VBJH,  $\text{mL g}^{-1}$ ) and metal loading (wt%, measured by ICP/AES) of different metal loaded nanostructures

Material	Surface area ( $S_{\text{BET}}$ , $\text{m}^2 \text{g}^{-1}$ )	Pore diameter ( $D_{\text{BJH}}$ , nm)	Pore volume ( $V_{\text{BJH}}$ , $\text{mL g}^{-1}$ )	Metal content (wt%)
Fe-MINT	97	<2	0.38	0.49
Fe-NT	181	<2	0.21	0.54
Cu-MINT	586	<2	0.25	0.51
Copper-NT	192	<2	0.20	0.55
Ni-MINT	165	<2	0.43	0.42
Ru-MINT	88	<2	0.26	0.58

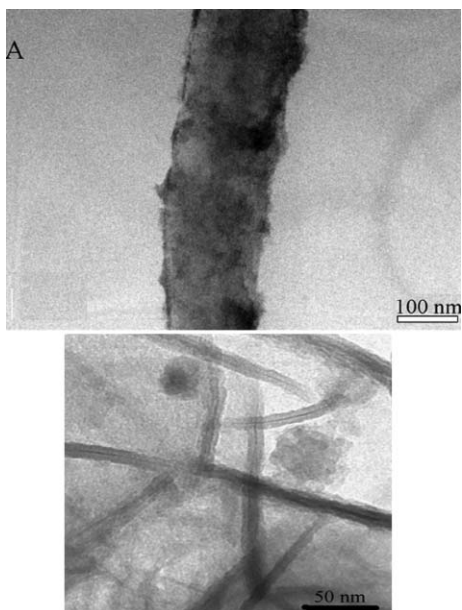


**Fig. 2** TEM micrographs of A) Ni-MINT; B) Cu-MINT (bottom) nanostructures.

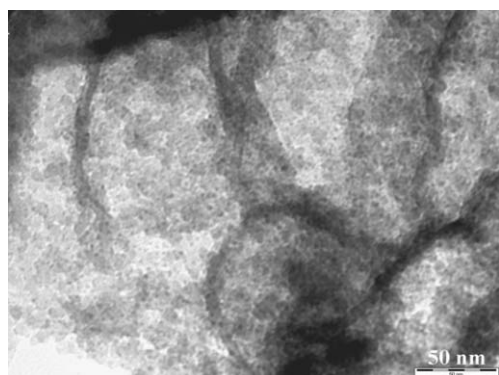


**Fig. 3** TEM micrographs of Cu-MINT material. Nanoparticles can be clearly seen as small dark spots present within the nanostructure.

Having proved the successful formation of nanotubular structures under microwave irradiation, the next step was to further broaden the scope of the protocol trying to prepare similar nanotubes under conventional heating.

TEM micrographs of such investigations demonstrated analogous nanotubular arrays could be successfully prepared under conventional heating using Fe and Cu chlorides (Fig. 4B). Nevertheless, significantly longer times of heating (1 h and over) were required to obtain similarly developed nanostructures with

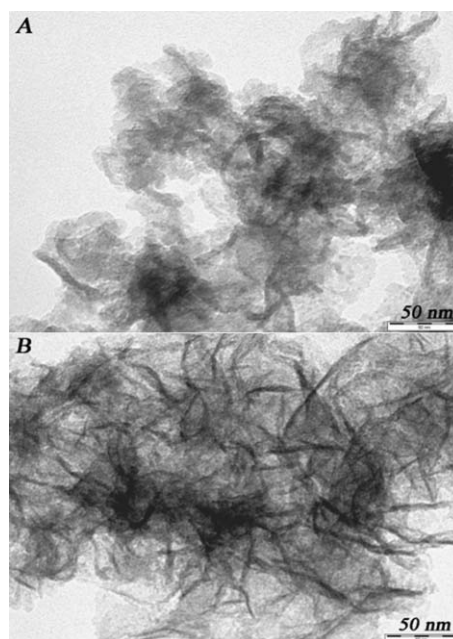


**Fig. 4** TEM micrographs of A) Fe-MINT prepared under microwave irradiation (200 W, 60–100 °C, 15 min) compared to B) Fe-NT prepared under conventional heating (70 °C, 2 h).

respect to those found under microwave irradiation (1–15 min). In contrast, typically reported spherical particle morphologies were observed when no metal chlorides were added to the synthesis methodology under the same conditions (both microwave irradiation and conventional heating, Fig. 5A). These findings pointed to the direct involvement of metal chlorides in the formation of such nanostructures.

Table 1 summarises the textural properties of the investigated materials. All nanotubular structures were found to have high surface areas (90–500  $\text{m}^2 \text{g}^{-1}$ ), being mostly microporous in nature (Table 1) regardless of the methodology employed for their synthesis.

Of note was the significantly higher surface area of Cu-MINT compared to other nanomaterials. This interesting fact is related to the inherent superior microporosity present in this material that can be clearly demonstrated in the nitrogen absorption/desorption curves included in Fig. 6.

Cu-MINT isotherm (Fig. 6, top) is completely different to those obtained, with similar profiles, for Fe-MINT and Cu and Fe-NT (Fig. 6, bottom), showing a remarkably superior microporosity that is likely to be the case for the increase of the surface area. It is well-known that an increase in the microporosity of the materials considerably increases their surface areas (e.g. micro-mesoporous carbons, zeolites and so on).<sup>16</sup> However, there may be other reasons for such difference in surface areas and microporosity that will be discussed in more detail later on.

According to all obtained results, in particular to the influence of the metal and precursor in the formation of the nanostructures, there were two key parameters which could also influence the generation of nanotubes that needed further investigation. These are the formation of supported nanoparticles that could act as *in situ* generated catalytic seeds to build-up the nanotube network and the anions from the metal precursor.



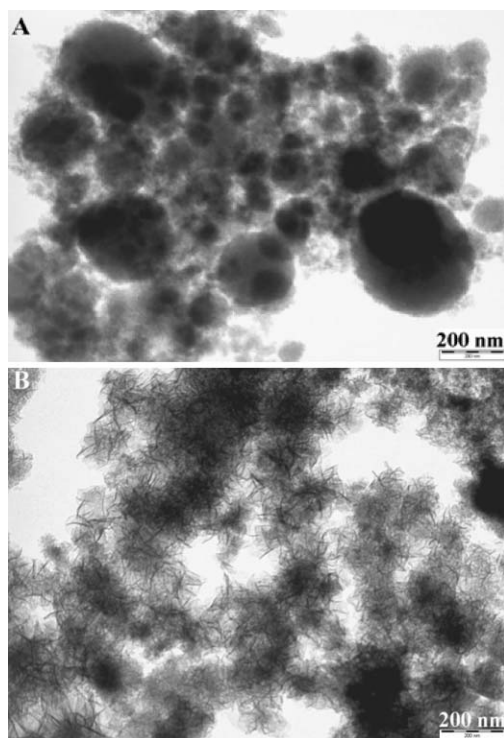


**Fig. 5** TEM micrographs of materials prepared under A) under microwave irradiation (200 W, 60–100 °C, 15 min) in the absence of a metal precursor compared to B) Fe-MINT under the same conditions prepared using  $\text{FeCl}_2$  as a metal precursor.

An interesting difference in the oxidation state of metal/metal oxide nanoparticles was also observed in the materials regardless of the type of metal. XPS spectra showed a significant shift in the XPS bands that corresponded to a higher content of reduced copper species in the Cu-MINT materials compared to the copper nanotubes (Table 2).<sup>10</sup> This evidence correlated well with the more developed nanotubes in Cu-MINT with respect to copper nanotubes. Interestingly, the relatively similar content of metallic Fe in both Fe-MINT and Fe-NT was in good agreement with relatively similar nanotubes developed for both materials (Table 2).<sup>10</sup> In the particular case of Ni materials, reduced species were only present at relatively low proportions as compared to  $\text{Ni}^{2+}$  species (possibly NiO).

**Table 2** Data of XP spectra [reduced and non reduced species (% of total metal content in the materials) as well as their corresponding bands] for different metal loaded nanostructures

Material	Reduced species (%)	Non reduced species (metal oxides)
Fe-MINT	12 ( $\text{Fe}^0$ , 706.2 eV)	86 (hematite, $\text{Fe}_2\text{O}_3$ )
Fe-NT	6 ( $\text{Fe}^0$ , 706.5 eV)	94 (hematite, $\text{Fe}_2\text{O}_3$ )
Cu-MINT	60 <sup>a</sup> (932.8 eV)	40 ( $\text{CuO}$ , 940–945 eV shake-up peak)
Copper-NT	15 <sup>a</sup> (933.0 eV)	85 ( $\text{CuO}$ , 940–945 eV shake-up peak)
Ni-MINT	45 ( $\text{Ni}^0$ , 852.6 eV)	55 ( $\text{Ni}^{2+}$ , 855.8 eV)
Ni-NT	28 ( $\text{Ni}^0$ , 853.1 eV)	72 ( $\text{Ni}^{2+}$ , 856.3 eV)

<sup>a</sup> Including  $\text{Cu}^0$  and  $\text{Cu}_2\text{O}$  as these species can only be distinguished by examination of their Auger spectra.<sup>17</sup>

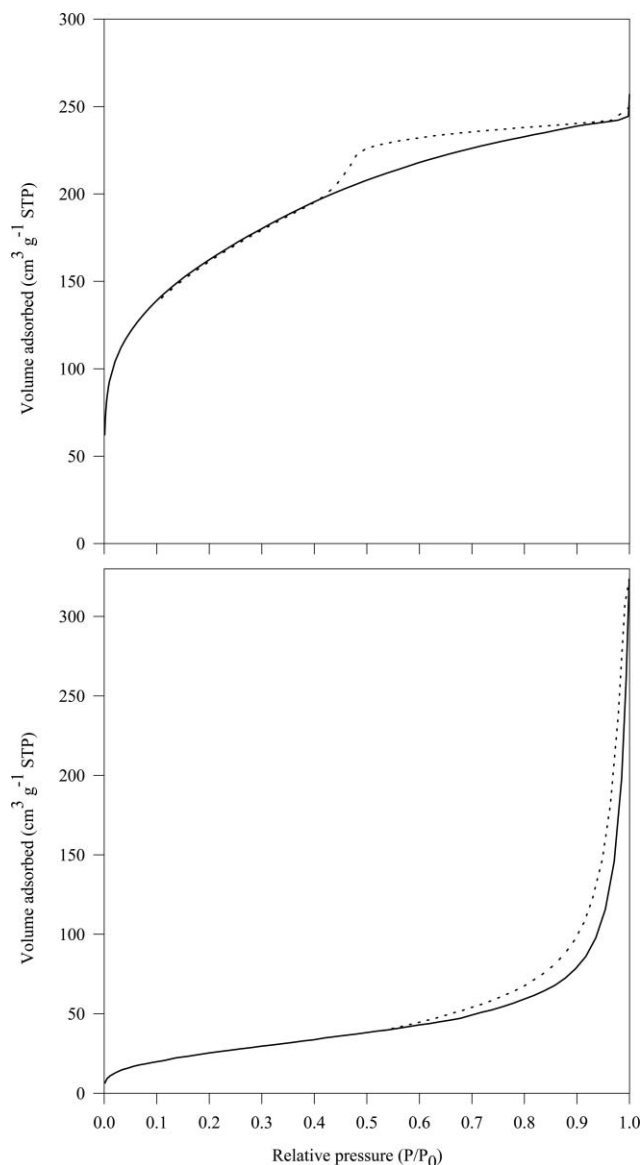


**Fig. 6** Isotherm profiles of Cu-MINT (top) and copper-NT (bottom).

However, the nature of the anions in the metal precursor were found to be the critical parameter in the formation of nanostructures. While the presence of halides [*e.g.*  $\text{Cl}^-$  (Fig. 2, Fig. 3, Fig. 4 and Fig. 7) and to a lesser extent  $\text{Br}^-$  (Fig. 7A) and  $\text{I}^-$  (Fig. 7D)] had a clear effect in the formation of nanorod/nanofibre-like domains, other anions including carbonates (Fig. 7B), sulfates (Fig. 7C), and even acetates rendered typical materials with spherical morphologies as well as heterogeneous structures (Fig. 7).

The generation of tubular nanostructures under the investigated conditions is therefore a complex process in which many different parameters seem to be involved. Nevertheless, based on further studies of these systems, we can propose two plausible mechanisms for the formation of nanotubular/fibre domains in the materials. These are based on several facts that were observed as follows:

-The addition of metal salts (*e.g.*  $\text{CuCl}_2$ ,  $\text{FeCl}_2$ ) to a *n*-dodecylamine/water/ACN solution causes an immediate

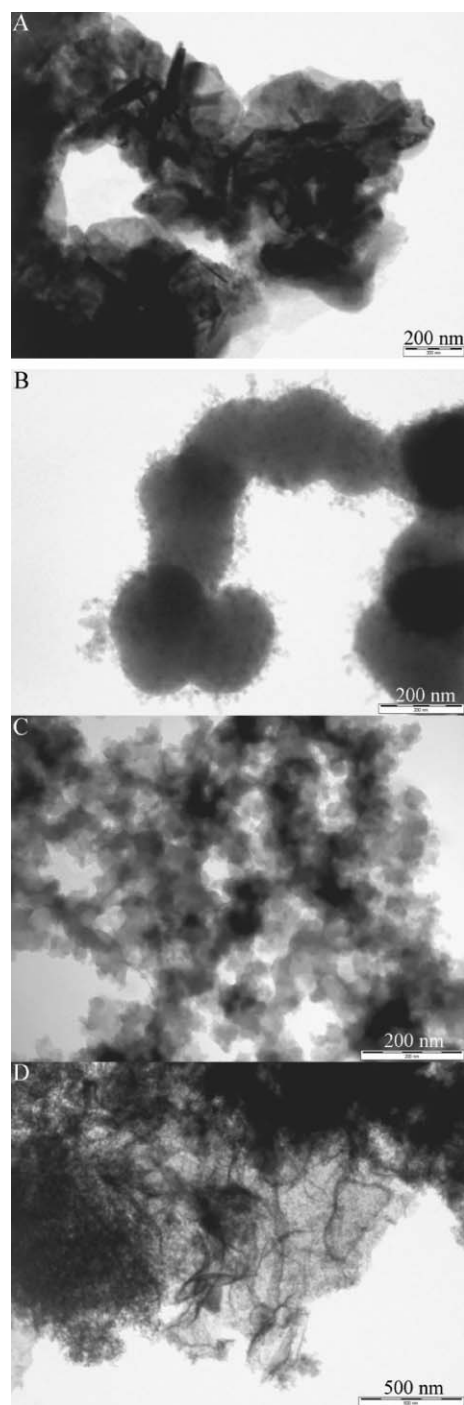


**Fig. 7** TEM micrographs of materials prepared using A)  $\text{CuBr}_2$ ; B)  $\text{CuCO}_3$ ; C)  $\text{CuSO}_4$  and D)  $\text{CuI}$  under conventional heating (2 h,  $70^\circ\text{C}$ ).

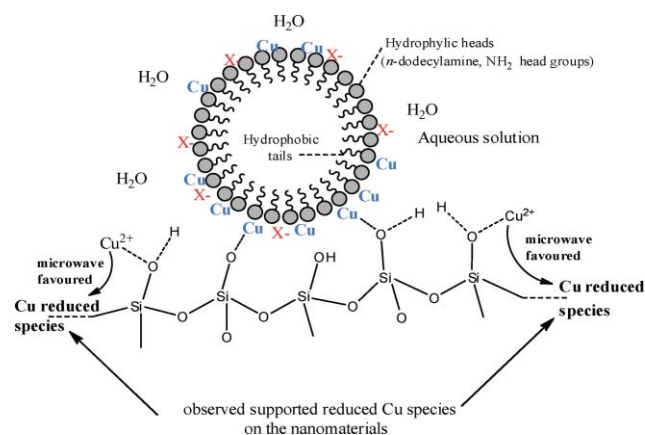
precipitate to form (blue and dark orange for the case of Cu and Fe, respectively).

-The precipitate formed is not soluble in ethanol at room temperature, which again points to the strong interaction between Cu and/or Fe to the amine.

-Surprisingly, the colour of the precipitate also changes when the pH is raised (by adding small quantities of  $\text{NaHCO}_3\text{-CO}_2$  given off), which might suggest that there may be a formation of some oxidic species containing amine ligands, and the effect is not just due to the amine changing the pH.

In fact, oxide surfaces can be very versatile ligands and thus we believe properties in our system can be described in the framework of coordination chemistry.

The first proposed mechanism (Scheme 1) is the coordination of the metal/metal oxide to the *n*-dodecylamine to give  $\text{ML}_n\text{X}$  complexes (where L is the amine and X are the halides). This coordination will increase the charge density of the micelles when formed, making them straighter. Furthermore, metal coordination to the head group of the micelle would increase its head volume, resulting in a dramatic shrinkage of the micelle, hence no mesopores will be observed, in good agreement with the porosity data obtained for the microporous materials (Table 1). Likewise, metal species may strongly interact with the silica precursor that will polymerise around the micelles to give the observed individual cylindrical-like nanotubes (*cf.* MCM-41 channels). However, a switch in the mechanism of hydrolysis cannot be ruled out.



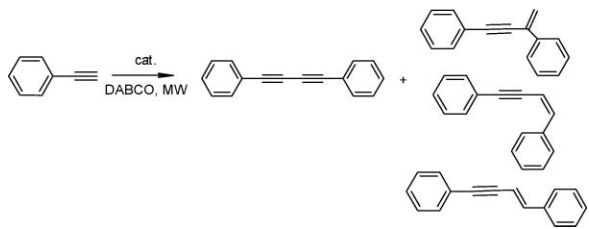
**Scheme 1** Proposed mechanism of formation of tubular nanostructures with different possibilities of interaction including the reduction of  $\text{M}^{2+}$  (in this example  $\text{Cu}^{2+}$ ) by OH groups on the surface of the material promoted by microwave irradiation.

The anions seemed also to have an important effect in the formation of the nanostructures. We believe the halides may also coordinate/bind (that is the reason of the proposed  $\text{ML}_n\text{X}$ ) and modify the structure of the complexes, and therefore the silica, whereas the other anions do not coordinate/bind (as much). In this regard, the order of coordination will be  $\text{Cl}^- > \text{Br}^- > \text{I}^-$ , that will correlate well with the size of the anion (bigger electronic cloud  $\text{I}^-$  anions will not coordinate/bind as well as smaller  $\text{Cl}^-$  anions).

With regards to the observation of metal nanoparticles, the hydroxyl groups on the silicate material have been reported to reduce metal ions in solution, and this process is favoured by gentle heating.<sup>18</sup> Thus, the differences in reduced nanoparticle species found between MINT and NT materials can be attributed to the fast and homogeneous heating achieved under microwave irradiation,<sup>19</sup> as well as its demonstrated improved reducing properties compared to conventional heating on solution containing metals.<sup>13,14,18</sup>

Another alternative lies in the idea that the  $\text{ML}_n\text{X}$  complex is not the structure directing agent, and the precipitate found in the absence of TEOS could be functioning as a template in the

**Table 3** Catalytic performance [total conversion and selectivity to homocoupling product ( $S_{\text{homocoupling}}$ )] of M-MINT and M-NT materials in the homocoupling of phenylacetylene under microwave irradiation<sup>a</sup>



Entry	Catalyst	Time/min	Conversion (mol%)	$S_{\text{homocoupling}}$ (mol%)
1	No catalyst	60	—	—
2	Conventional silica	60	—	—
3	CuI (5 mol%) <sup>b</sup>	30	30	>99
3	Fe-MINT	30	<30	>99
4	Fe-NT	30	<20	>99
5	Cu-MINT	30	>90	75 <sup>c</sup>
6	Copper-NT	30	80	85 <sup>c</sup>
7	Ni-MINT	15	>95	70 <sup>c</sup>
8	Ru-MINT	30	<10	>99

<sup>a</sup> Reaction conditions: 4 mmol phenylacetylene, 2 mmol DABCO, 0.05 g catalyst, 300 W, 140–170 °C. <sup>b</sup> Neat CuI was employed as catalyst. <sup>c</sup> The difference to 100 corresponds to the formation of enynes.

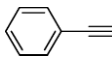
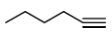
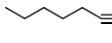
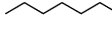
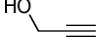
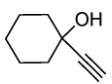
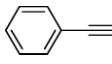
solid state or even reorganising under microwave/conventional heating to reform the amine and then templating.

With regards to the potential application of the prepared nanomaterials, materials from this work were tested in the microwave-assisted homocoupling of terminal alkynes. Coupling processes have recently received a great deal of attention as highly desirable protocols in organic synthesis.<sup>20–22</sup> Among them, alkyne homocoupling or dimerisation to 1,3-diynes is particularly important in the synthesis of a wide chemical spectra ranging from natural products to polymers.<sup>23</sup> However, most reported systems for these homocoupling processes involve homogeneous conditions and employ metal salts and/or complexes including Pd,<sup>20,22,24</sup> Cu<sup>25</sup> and/or Ni<sup>26</sup> as well as Ru,<sup>27</sup> with only few truly heterogeneously catalysed protocols having been reported up to date dealing with highly active and/or reusable heterogeneous Pd<sup>28</sup> or Cu<sup>29</sup> systems.

Recent reports highlighted the possibility of using Ni-based protocols for the effective oxidative coupling of terminal alkynes promoted by oxygen or air,<sup>26,30</sup> in good agreement with our latest results on alkyne homocoupling catalysed reactions by supported Ni(II) complexes on biopolymers (*e.g.* chitosan).<sup>31</sup> This reaction seems to be promoted by Ni<sup>2+</sup> species and a remarkable increase to the homocoupling products was observed when CuI was added as co-catalyst.<sup>26,31</sup>

Results obtained for the M-MINT and M-NT materials in the heterogeneously-catalysed homocoupling of phenylacetylene under microwave irradiation have been included in Table 3. The conventionally heated reaction progressed smoothly to give complete conversions and selectivity to the homocoupling product after 12–18 h reaction at 100 °C (not shown). Interestingly, the addition of small quantities of CuI in the absence of catalyst was found to be sufficient to achieve complete formation of the phenylacetylene dimer in 6–18 h depending on the quantity added of CuI (*e.g.* >95% conversion in 18 h employing 2 mol%

**Table 4** Catalytic performance of Ni-MINT in the microwave-assisted homocoupling of a range of terminal alkynes<sup>a</sup>

Entry	Substrate	Time/min	Conversion (mol%)	$S_{\text{homocoupling}}$ (mol%)
1		15	>95	70
2		30	>99(86)	>99
3		30	>99(90)	>99
4		30	>99(92)	>99
5		45	85	60
6		30	>90	80
Reused <sup>b</sup>		15	89	60

<sup>a</sup> Reaction conditions 4 mmol substrate, 2 mmol DABCO, 0.05 g catalyst, microwaves, 300 W, 140–170 °C. <sup>b</sup> Activity of reused recovered catalyst in the 4th reaction cycle. Isolated yields, where appropriate, are given in brackets.

CuI; >99% conversion in 12 h adding 10 mol% CuI at 100 °C). Comparatively, microwave-assisted reactions provided excellent conversions of starting materials for Cu and Ni nanomaterials, compared to the poor activity found for similar catalytic quantities of CuI (Table 3, entry 3). Fairly high selectivities to the homocoupling product were observed at very short times of reaction (typically 15–30 min) and low catalyst quantities. The main by-products in the reaction were the enynes showed in Table 3. Ni-MINT material appeared to be the most active in the reaction and a complete conversion to products could be obtained after 15 min of microwave irradiation. Ni<sup>2+</sup> species in the Ni-materials are likely to be responsible for the activity in the systems but more detailed studies are required to unravel the mechanism of the reaction and its similarity (or not) as compared to the reported homogeneous systems.<sup>26,30</sup>

The scope of the protocol was then extended to a range of terminal alkynes for the most active Ni-MINT material as shown in Table 4. Quantitative conversion and selectivity to the corresponding homocoupling products were obtained under the investigated reaction conditions (Table 4), generally short times of irradiation (<30 min) and low catalyst quantities (0.05 g).

Microwave irradiation reduced the times of reaction needed for reaction completion from 6–18 h (under conventional heating) to a few minutes (15–30 min). The methodology was therefore amenable to a wide range of substrates and substituents under mild reaction conditions.

Most importantly the catalyst was also highly recyclable under the investigated conditions, preserving almost 90% of its initial activity and selectivity after 3 reuses (Table 4, entry 1 vs. reused). These materials have also been compared to similar literature reports (Table 5). While the majority of the reports to date deal with conventionally heated systems that required long times of reaction (>3 h), our system allowed quantitative conversion

**Table 5** Comparison of the catalytic performance of state-of-the-art catalysts with the reported metal-MINT systems in the homocoupling of phenylacetylene under similar reaction conditions

Reference	Reaction conditions	Time/min	Conversion (mol%)
This work	4 mmol substrate, 0.05 g Ni-MINT (5 mol% Ni), 2 mmol DABCO, 300 W, 170 °C, microwaves	15	>95
This work	4 mmol substrate, 0.05 g Cu-MINT (6 mol% Cu), 2 mmol DABCO, 300 W, 160 °C, microwaves	30	>90
25a	5 mmol substrate, 2 mol% CuCl, 10 mol% piperidine, 60 °C, conventional heating	300	96
25c	1 mmol substrate, 1 mmol CuI, 1 mmol I <sub>2</sub> , 2 mmol Na <sub>2</sub> CO <sub>3</sub> , 80 °C, conventional heating	180	99
25d	1 mmol substrate, 4.4 mol% Cu, O <sub>2</sub> , 100 °C, conventional heating	180	91
26	2 mmol substrate, 1 equiv. n-BuLi, 1 equiv. NiCl <sub>2</sub> .DME, 2 equiv. CuI, 80 °C, conventional heating	60	>99
29c	1 mmol substrate, 30 mol% Cu-USY zeolite, no base, 110 °C, conventional heating	900	97

and selectivity to the corresponding diyne in 15–30 min under microwave irradiation conditions. The reported work describes a novel family of nanomaterials that give comparable and/or improved activities to those already reported at comparatively shorter reaction times and catalyst loadings (Table 5). This also constitutes the first report to date of a highly active and reusable heterogeneously Ni catalysed homocoupling of terminal alkynes under microwave irradiation.

## Conclusions

Self-assembled tubular nanostructures can be prepared from aqueous surfactant-mediated systems both under conventional heating and microwave irradiation. Further studies about the effect of the anions/cations, metal nanoparticles, porosity and structural properties showed such nanostructures may be generated through the coordination of the metals (Cu, Fe, Ni) and/or halides to the amine (ML<sub>n</sub>X complexes) in the liquid phase thus influencing the formation of straighter micelles that lead to microporous materials or alternatively *via* ML<sub>n</sub>X templating in the solid state/restructured material under microwave irradiation. In any case, the MINT/NT materials were found to have interesting catalytic properties and were proved to be very active and selective in the microwave-assisted homocoupling of terminal alkynes. We envisage the supported systems can greatly contribute to advance the development of active and selective supported materials owing to their wide availability, ease of preparation and low cost as well as promoting the green credentials of future catalytic protocols in terms of sustainability and environmentally friendliness.

## Acknowledgements

CG-A would like to thank Ministerio de Educación y Ciencia and Fundación Española para la Ciencia y Tecnología for a funded fellowship and Ministerio de Ciencia e Innovación for a Ramon y Cajal contract (ref RYC-2010-06268). RL is also grateful to Ministerio de Ciencia e Innovación, Gobierno de

España for the provision of a Ramon y Cajal contract (ref RYC-2009-04199). AMB and RLA gratefully acknowledge current funding from projects P09-FQM-4781 and CTQ2008-01330.

## Notes and references

- 1 Y. Cui, Q. Q. Wei, H. K. Park and C. M. Lieber, *Science*, 2001, **293**, 1289–1292.
- 2 H. M. Fan, J. B. Yi, Y. Yang, K. W. Kho, H. R. Tan, Z. X. Shen, J. Ding, X. W. Sun, M. C. Olivo and Y. P. Feng, *ACS Nano*, 2009, **3**, 2798–2808.
- 3 Y. Huang, X. F. Duan and C. M. Lieber, *Small*, 2005, **1**, 142–147.
- 4 (a) A. G. S. Prado and L. L. Costa, *J. Hazard. Mater.*, 2009, **169**, 297–301; (b) C. J. Lin, W. Y. Yun, Y. T. Lu and S. H. Chien, *Chem. Commun.*, 2008, 6031–6033.
- 5 J. T. Hu, T. W. Odom and C. M. Lieber, *Acc. Chem. Res.*, 1999, **32**, 435–445.
- 6 F. D. Wang, A. G. Dong, J. W. Sun, R. Tang, H. Yu and W. E. Buhro, *Inorg. Chem.*, 2006, **45**, 7511–7521.
- 7 P. S. Shah, T. Hanrah, K. P. Johnston and B. A. Korgel, *J. Phys. Chem. B*, 2004, **108**, 9574–9587.
- 8 H. P. Lin, C. Y. Mou and S. B. Liu, *Adv. Mater.*, 2000, **12**, 103–106.
- 9 (a) D. C. Lee, F. V. Mikulec and B. A. Korgel, *J. Am. Chem. Soc.*, 2004, **126**, 4951–4957; (b) D. K. Smith, D. C. Lee and B. A. Korgel, *Chem. Mater.*, 2006, **18**, 3356–3364; (c) H. Y. Tuan, A. Ghezalbach and B. A. Korgel, *Chem. Mater.*, 2008, **20**, 2306–2313.
- 10 C. Gonzalez-Arellano, R. Luque and D. J. Macquarrie, *Chem. Commun.*, 2009, 4581–4583.
- 11 (a) N. Y. Hsu, C. C. Chien and K. T. Jeng, *Appl. Catal., B*, 2008, **84**, 196–203; (b) L. M. Sikhwivhilu, S. S. Ray and N. J. Coville, *Diffusion Defect Data–Solid State Phenomena*, 2008, **140**, 61–68.
- 12 (a) X. Pan and X. Bao, *Chem. Commun.*, 2008, 6271–6281; (b) W. Chen, Z. Fan, X. Pan and X. Bao, *J. Am. Chem. Soc.*, 2008, **130**, 9414–9419.
- 13 J. M. Campelo, T. D. Conesa, M. J. Gracia, M. J. Jurado, R. Luque, J. M. Marinas and A. A. Romero, *Green Chem.*, 2008, **10**, 853–858.
- 14 C. González-Arellano, J. M. Campelo, D. J. Macquarrie, J. M. Marinas, A. A. Romero and R. Luque, *ChemSusChem*, 2008, **1**, 746–750.
- 15 D. J. Macquarrie, B. C. Gilbert, L. J. Gilbert, A. Caragheorghopol, F. Savonea, D. B. Jackson, B. Onida, E. Garrone and R. Luque, *J. Mater. Chem.*, 2005, **15**, 3946–3951.
- 16 (a) V. Budarin, J. H. Clark, J. J. E. Hardy, R. Luque, K. Millkowski, S. Tavener and A. Wilson, *Angew. Chem., Int. Ed.*, 2006, **45**, 3782–3786; (b) W. Liu, Y. Soneda, M. Kodama, J. Yamashita and H. Hatori, *Mater. Lett.*, 2008, **62**, 2766–2768; (c) D. Carriazo, S. Lima,



- C. Martin, M. Pillinger, A. A. Valente and V. Rives, *J. Phys. Chem. Solids*, 2007, **68**, 1872–1880.
- 17 Z. W. Huang, F. Cui, H. X. Kang, J. Chen, X. Z. Zhang and C. G. Xia, *Chem. Mater.*, 2008, **20**, 5090–5099.
- 18 (a) T. Tuval and A. Gedanken, *Nanotechnology*, 2007, **18**, 255601; (b) P. Mukherjee, C. R. Patra, A. Ghosh, R. Kumar and M. Sastry, *Chem. Mater.*, 2002, **14**, 1678–1684.
- 19 C. O. Kappe, *Chem. Soc. Rev.*, 2008, **37**, 1127–1139.
- 20 *Handbook of organopalladium chemistry for organic synthesis*, ed. E. Negishi, 1st edn, Wiley-Interscience, New York, 2002.
- 21 *Handbook of C-H transformations*, Ed. G. Dyker, 1st edn, Wiley-VCH, Weinheim, 2005.
- 22 J. Tsuji, *Palladium reagents and catalysts: new perspectives for the 21st century*, 1st edn, John Wiley & Sons, Chichester, 2004.
- 23 (a) J. M. Tour, *Chem. Rev.*, 1996, **96**, 537–553; (b) R. E. Martin and F. Diederich, *Angew. Chem., Int. Ed.*, 1999, **38**, 1350–1377.
- 24 (a) P. Siemsen, B. Felber, *Handbook of C-H transformations*, Ed. G. Dyker, 1st edn, Wiley-VCH, Weinheim, 2005, 53–62, 83–84; (b) A. S. Batsanov, J. C. Collings, I. J. S. Fairlamb, J. P. Holland, J. A. K. Howard, Z. Y. Lin, T. B. Marder, A. C. Parsons, R. M. Ward and J. Zhu, *J. Org. Chem.*, 2005, **70**, 703–706.
- 25 (a) Q. Zheng, R. Hua and Y. Wan, *Appl. Organomet. Chem.*, 2010, **24**, 314–316; (b) S. Adimurthy, C. C. Malakar and U. Beifuss, *J. Org. Chem.*, 2009, **74**, 5648–5651; (c) D. F. Li, K. Yin, J. Li and X. S. Jia, *Tetrahedron Lett.*, 2008, **49**, 5918–5919; (d) K. Kamata, S. Yamaguchi, M. Kotani, K. Yamaguchi and N. Mizuno, *Angew. Chem., Int. Ed.*, 2008, **47**, 2407–2410.
- 26 J. D. Crowley, S. M. Goldup, N. D. Gowans, D. A. Leigh, V. E. Ronaldson and A. M. Z. Slawin, *J. Am. Chem. Soc.*, 2010, **132**, 6243–6248.
- 27 K. Melis, D. De Vos, P. Jacobs and F. Verpoort, *J. Organomet. Chem.*, 2003, **671**, 131–136.
- 28 S. N. Chen, W. Y. Wu and F. Y. Tsai, *Green Chem.*, 2009, **11**, 269–274.
- 29 (a) D. Wang, J. H. Li, N. Li, T. T. Gao, S. H. Hou and B. H. Chen, *Green Chem.*, 2010, **12**, 45–48; (b) T. Oishi, T. Katayama, K. Yamaguchi and N. Mizuno, *Chem.–Eur. J.*, 2009, **15**, 7539–7542; (c) P. Kuhn, A. Alix, M. Kumarraja, B. Louis, P. Pale and J. Sommer, *Eur. J. Org. Chem.*, 2009, 423–429.
- 30 W. Y. Yin, C. He, M. Chen, H. Zhang and A. W. Lei, *Org. Lett.*, 2009, **11**, 709–712.
- 31 R. Luque, unpublished results.